

University of Nebraska - Lincoln

DigitalCommons@University of Nebraska - Lincoln

Gregory Snow Publications

Research Papers in Physics and Astronomy

November 2007

Search for a Higgs boson produced in association with a Z boson in $p\bar{p}$ collisions

V. M. Abazov

Joint Institute for Nuclear Research, Dubna, Russia

Kenneth A. Bloom

University of Nebraska - Lincoln, kbloom2@unl.edu

Gregory Snow

University of Nebraska - Lincoln, gsnow1@unl.edu

Follow this and additional works at: <https://digitalcommons.unl.edu/physicsnow>



Part of the [Physics Commons](#)

Abazov, V. M.; Bloom, Kenneth A.; and Snow, Gregory, "Search for a Higgs boson produced in association with a Z boson in $p\bar{p}$ collisions" (2007). *Gregory Snow Publications*. 31.

<https://digitalcommons.unl.edu/physicsnow/31>

This Article is brought to you for free and open access by the Research Papers in Physics and Astronomy at DigitalCommons@University of Nebraska - Lincoln. It has been accepted for inclusion in Gregory Snow Publications by an authorized administrator of DigitalCommons@University of Nebraska - Lincoln.

Search for a Higgs boson produced in association with a Z boson in $p\bar{p}$ collisions

DØ Collaboration

V.M. Abazov^{ai}, B. Abbott^{bw}, M. Abolins^{bm}, B.S. Acharya^{ab}, M. Adams^{ay}, T. Adams^{aw}, E. Aguilo^e, S.H. Ahn^{ad}, M. Ahsan^{bg}, G.D. Alexeev^{ai}, G. Alkhazov^{am}, A. Alton^{bl, 1}, G. Alverson^{bk}, G.A. Alves^b, M. Anastasoia^{ah}, L.S. Ancu^{ah}, T. Andeen^{ba}, S. Anderson^{as}, B. Andrieu^p, M.S. Anzelc^{ba}, Y. Arnoud^m, M. Arov^{bh}, M. Arthaud^q, A. Askew^{aw}, B. Åsman^{an}, A.C.S. Assis Jesus^c, O. Atramentov^{aw}, C. Autermann^t, C. Avila^g, C. Ay^w, F. Badaud^l, A. Baden^{bi}, L. Bagby^{az}, B. Baldin^{ax}, D.V. Bandurin^{bg}, P. Banerjee^{ab}, S. Banerjee^{ab}, E. Barberis^{bk}, A.-F. Barfussⁿ, P. Bargassa^{cb}, P. Baringer^{bf}, J. Barreto^b, J.F. Bartlett^{ax}, U. Bassler^p, D. Bauer^{aq}, S. Beale^e, A. Bean^{bf}, M. Begalli^c, M. Begel^{bs}, C. Belanger-Champagne^{an}, L. Bellantoni^{ax}, A. Bellavance^{ax}, J.A. Benitez^{bm}, S.B. Beri^z, G. Bernardi^p, R. Bernhard^v, L. Berntzonⁿ, I. Bertram^{ap}, M. Besançon^q, R. Beuselinck^{aq}, V.A. Bezzubov^{al}, P.C. Bhat^{ax}, V. Bhatnagar^z, C. Biscarat^s, G. Blazey^{az}, F. Blekman^{aq}, S. Blessing^{aw}, D. Bloch^r, K. Bloom^{bo}, A. Boehnlein^{ax}, D. Boline^{bj}, T.A. Bolton^{bg}, G. Borissov^{ap}, K. Bos^{ag}, T. Bose^{by}, A. Brandt^{bz}, R. Brock^{bm}, G. Brooijmans^{br}, A. Bross^{ax}, D. Brown^{bz}, N.J. Buchanan^{aw}, D. Buchholz^{ba}, M. Buehler^{cc}, V. Buescher^u, S. Burdin^{ap, 2}, S. Burke^{as}, T.H. Burnett^{cd}, C.P. Buszello^{aq}, J.M. Butler^{bj}, P. Calfayan^x, S. Calvetⁿ, J. Cammin^{bs}, S. Caron^{ag}, W. Carvalho^c, B.C.K. Casey^{by}, N.M. Cason^{bc}, H. Castilla-Valdez^{af}, S. Chakrabarti^q, D. Chakraborty^{az}, K. Chan^e, K.M. Chan^{bc}, A. Chandra^{av}, F. Charles^r, E. Cheu^{as}, F. Chevallier^m, D.K. Cho^{bj}, S. Choi^{ae}, B. Choudhary^{aa}, L. Christofek^{by}, T. Christoudias^{aq}, S. Cihangir^{ax}, D. Claes^{bo}, B. Clément^f, C. Clément^{an}, Y. Coadou^e, M. Cooke^{cb}, W.E. Cooper^{ax}, M. Corcoran^{cb}, F. Couderc^q, M.-C. Cousinouⁿ, S. Crépe-Renaudin^m, D. Cutts^{by}, M. Cwiok^{ac}, H. da Motta^b, A. Das^{bj}, G. Davies^{aq}, K. De^{bz}, P. de Jong^{ag}, S.J. de Jong^{ah}, E. De La Cruz-Burelo^{bl}, C. De Oliveira Martins^c, J.D. Degenhardt^{bl}, F. Déliot^q, M. Demarteau^{ax}, R. Demina^{bs}, D. Denisov^{ax}, S.P. Denisov^{al}, S. Desai^{ax}, H.T. Diehl^{ax}, M. Diesburg^{ax}, A. Dominguez^{bo}, H. Dong^{bt}, L.V. Dudko^{ak}, L. Duflot^o, S.R. Dugad^{ab}, D. Duggan^{aw}, A. Duperrinⁿ, J. Dyer^{bm}, A. Dyshkant^{az}, M. Eads^{bo}, D. Edmunds^{bm}, J. Ellison^{av}, V.D. Elvira^{ax}, Y. Enari^{by}, S. Eno^{bi}, P. Ermolov^{ak}, H. Evans^{bb}, A. Evdokimov^{bu}, V.N. Evdokimov^{al}, A.V. Ferapontov^{bg}, T. Ferbel^{bs}, F. Fiedler^x, F. Filthaut^{ah}, W. Fisher^{ax}, H.E. Fisk^{ax}, M. Ford^{ar}, M. Fortner^{az}, H. Fox^v, S. Fu^{ax}, S. Fuess^{ax}, T. Gadfort^{cd}, C.F. Galea^{ah}, E. Gallas^{ax}, E. Galyaev^{bc}, C. Garcia^{bs}, A. Garcia-Bellido^{cd}, V. Gavrilov^{aj}, P. Gay^l, W. Geist^f, D. Gelé^r, C.E. Gerber^{ay}, Y. Gershtein^{aw}, D. Gillberg^e, G. Ginther^{bs}, N. Gollub^{an}, B. Gómez^g, A. Goussiou^{bc}, P.D. Grannis^{bt}, H. Greenlee^{ax}, Z.D. Greenwood^{bh}, E.M. Gregores^d, G. Grenier^s, Ph. Gris^l, J.-F. Grivaz^o, A. Grohsjean^x, S. Grünendahl^{ax}, M.W. Grünewald^{ac}, F. Guo^{bt}, J. Guo^{bt}, G. Gutierrez^{ax}, P. Gutierrez^{bw}, A. Haas^{br}, N.J. Hadley^{bi}, P. Haefner^x, S. Hagopian^{aw}, J. Haley^{bp}, I. Hall^{bw}, R.E. Hall^{au}, L. Han^f, K. Hanagaki^{ax}, P. Hansson^{an}, K. Harder^{ar}, A. Harel^{bs}, R. Harrington^{bk}, J.M. Hauptman^{be}, R. Hauser^{bm}, J. Hays^{aq}, T. Hebbeker^t, D. Hedin^{az}, J.G. Hegeman^{ag}, J.M. Heinmiller^{ay}, A.P. Heinson^{av}, U. Heintz^{bj}, C. Hensel^{bf}, K. Herner^{bt}, G. Hesketh^{bk}, M.D. Hildreth^{bc}, R.

Hirosky^{cc}, **J.D. Hobbs**^{bt,*}, B. Hoeneisen^k, H. Hoeth^y, M. Hohlfeld^u, S.J. Hong^{ad}, R. Hooper^{by}, S. Hossain^{bw}, P. Houben^{ag}, Y. Hu^{bt}, Z. Hubacekⁱ, V. Hynek^h, I. Iashvili^{bq}, R. Illingworth^{ax}, A.S. Ito^{ax}, S. Jabeen^{bj}, M. Jaffré^o, S. Jain^{bw}, K. Jakobs^v, C. Jarvis^{bi}, R. Jesik^{aq}, K. Johns^{as}, C. Johnson^{br}, M. Johnson^{ax}, A. Jonckheere^{ax}, P. Jonsson^{aq}, A. Juste^{ax}, D. Käfer^t, S. Kahn^{bu}, E. Kajfaszⁿ, A.M. Kalinin^{ai}, J.M. Kalk^{bh}, J.R. Kalk^{bm}, S. Kappler^t, D. Karmanov^{ak}, J. Kasper^{bj}, P. Kasper^{ax}, I. Katsanos^{br}, D. Kau^{aw}, R. Kaur^z, V. Kaushik^{bz}, R. Kehoe^{ca}, S. Kermicheⁿ, N. Khalatyan^{al}, A. Khanov^{bx}, A. Kharchilava^{bq}, Y.M. Kharzheev^{ai}, D. Khatidze^{br}, H. Kim^{ae}, T.J. Kim^{ad}, M.H. Kirby^{ah}, M. Kirsch^t, B. Klima^{ax}, J.M. Kohli^z, J.-P. Konrath^v, M. Kopal^{bw}, V.M. Korablev^{al}, B. Kothari^{br}, A.V. Kozelov^{al}, D. Krop^{bb}, A. Kryemadhi^{cc}, T. Kuhl^w, A. Kumar^{bq}, S. Kunori^{bi}, A. Kupco^j, T. Kurča^s, J. Kvita^h, D. Lam^{bc}, S. Lammers^{br}, G. Landsberg^{by}, J. Lazoflores^{aw}, P. Lebrun^s, W.M. Lee^{ax}, A. Leflat^{ak}, F. Lehner^{ao}, J. Lellouch^p, V. Lesne^l, J. Leveque^{as}, P. Lewis^{aq}, J. Li^{bz}, L. Li^{av}, Q.Z. Li^{ax}, S.M. Lietti^d, J.G.R. Lima^{az}, D. Lincoln^{ax}, J. Linnemann^{bm}, V.V. Lipaev^{al}, R. Lipton^{ax}, Y. Liu^f, Z. Liu^e, L. Lobo^{aq}, A. Lobodenko^{am}, M. Lokajicek^j, A. Lounis^r, P. Love^{ap}, H.J. Lubatti^{cd}, A.L. Lyon^{ax}, A.K.A. Maciel^b, D. Mackin^{cb}, R.J. Madaras^{at}, P. Mättig^y, C. Magass^t, A. Magerkurth^{bl}, N. Makovec^o, P.K. Mal^{bc}, H.B. Malbouisson^c, S. Malik^{bo}, V.L. Malyshev^{ai}, H.S. Mao^{ax}, Y. Maravin^{bg}, B. Martin^m, R. McCarthy^{bt}, A. Melnitchouk^{bn}, A. Mendesⁿ, L. Mendoza^g, P.G. Mercadante^d, M. Merkin^{ak}, K.W. Merritt^{ax}, A. Meyer^t, J. Meyer^u, M. Michaut^q, T. Millet^s, J. Mitrevski^{br}, J. Molina^c, R.K. Mommsen^{ar}, N.K. Mondal^{ab}, R.W. Moore^e, T. Moulik^{bf}, G.S. Muanza^s, M. Mulders^{ax}, M. Mulhearn^{br}, O. Mundal^u, L. Mundim^c, E. Nagyⁿ, M. Naimuddin^{ax}, M. Narain^{by}, N.A. Naumann^{ah}, H.A. Neal^{bl}, J.P. Negret^g, P. Neustroev^{am}, H. Nilsen^v, C. Noeding^v, A. Nomerotski^{ax}, S.F. Novaes^d, T. Nunnemann^x, V. O'Dell^{ax}, D.C. O'Neil^e, G. Obrant^{am}, C. Ochando^o, D. Onoprienko^{bg}, N. Oshima^{ax}, J. Osta^{bc}, R. Otecⁱ, G.J. Otero y Garzón^{ay}, M. Owen^{ar}, P. Padley^{cb}, M. Pangilinan^{by}, N. Parashar^{bd}, S.-J. Park^{bs}, S.K. Park^{ad}, J. Parsons^{br}, R. Partridge^{by}, N. Parua^{bb}, A. Patwa^{bu}, G. Pawloski^{cb}, P.M. Perea^{av}, K. Peters^{ar}, Y. Peters^y, P. Pétrouff^o, M. Petteni^{aq}, R. Piegai^a, J. Piper^{bm}, M.-A. Pleier^u, P.L.M. Podesta-Lerma^{af,3}, V.M. Podstavkov^{ax}, Y. Pogorelov^{bc}, M.-E. Pol^b, A. Pompos^{gbw}, B.G. Pope^{bm}, A.V. Popov^{al}, C. Potter^e, W.L. Prado da Silva^c, H.B. Prosper^{aw}, S. Protopopescu^{bu}, J. Qian^{bl}, A. Quadt^u, B. Quinn^{bn}, A. Rakitine^{ap}, M.S. Rangel^b, K.J. Rani^{ab}, K. Ranjan^{aa}, P.N. Ratoff^{ap}, P. Renkel^{ca}, S. Reucroft^{bk}, P. Rich^{ar}, M. Rijssenbeek^{bt}, I. Ripp-Baudot^f, F. Rizatdinova^{bx}, S. Robinson^{aq}, R.F. Rodrigues^c, C. Royon^q, P. Rubinov^{ax}, R. Ruchti^{bc}, G. Safronov^{aj}, G. Sajot^m, A. Sánchez-Hernández^{af}, M.P. Sanders^p, A. Santoro^c, G. Savage^{ax}, L. Sawyer^{bh}, T. Scanlon^{aq}, D. Schaile^x, R.D. Schamberger^{bt}, Y. Scheglov^{am}, H. Schellman^{ba}, P. Schieferdecker^x, T. Schliephake^y, C. Schmitt^y, C. Schwanenberger^{ar}, A. Schwartzman^{bp}, R. Schwienhorst^{bm}, J. Sekaric^{aw}, S. Sengupta^{aw}, H. Severini^{bw}, E. Shabalina^{ay}, M. Shamim^{bg}, V. Shary^q, A.A. Shchukin^{al}, R.K. Shivpuri^{aa}, D. Shpakov^{ax}, V. Siccari^f, V. Simakⁱ, V. Sirotenko^{ax}, P. Skubic^{bw}, P. Slattery^{bs}, D. Smirnov^{bc}, R.P. Smith^{ax}, G.R. Snow^{bo}, J. Snow^{bv}, S. Snyder^{bu}, S. Söldner-Rembold^{ar}, L. Sonnenschein^p, A. Sopczak^{ap}, M. Sosebee^{bz}, K. Soustruznik^h, M. Souza^b, B. Spurlock^{bz}, J. Stark^m, J. Steele^{bh}, V. Stolin^{aj}, A. Stone^{ay}, D.A. Stoyanova^{al}, J. Strandberg^{bl}, S. Strandberg^{an}, M.A. Strang^{bq}, M. Strauss^{bw}, R. Ströhmer^x, D. Strom^{ba}, M. Strovink^{at}, L. Stutte^{ax}, S. Sumowidagdo^{aw}, P. Svoisky^{bc}, A. Sznajder^c, M. Talbyⁿ, P. Tamburello^{as}, A. Tanasijczuk^a, W. Taylor^e, P. Telford^{ar}, J. Temple^{as}, B. Tiller^x, F. Tissandier^l, M. Titov^q, V.V. Tokmenin^{ai}, M. Tomoto^{ax}, T. Toole^{bi}, I. Torchiani^v, T. Trefzger^w, D. Tsybychev^{bt}, B. Tuchming^q, C. Tully^{bp}, P.M. Tuts^{br}, R. Unalan^{bm}, L. Uvarov^{am}, S. Uvarov^{am}, S. Uzunyan^{az}, B. Vachon^e, P.J. van den Berg^{ag}, B. van Eijk^{ai}, R. Van Kooten^{bb}, W.M. van Leeuwen^{ag}, N. Varelas^{ay}, E.W. Varnes^{as}, A. Vartapetian^{bz}, I.A. Vasilyev^{al}, M. Vaupel^y, P. Verdier^s, L.S.

Vertogradov^{ai}, M. Verzocchi^{ax}, F. Villeneuve-Seguier^{aq}, P. Vint^{aq}, E. Von Toerne^{bg}, M. Voutilainen^{bo, 4}, M. Vreeswijk^{ag}, R. Wagner^{bp}, H.D. Wahl^{aw}, L. Wang^{bi}, M.H.L.S. Wang^{ax}, J. Warchol^{bc}, G. Watts^{cd}, M. Wayne^{bc}, G. Weber^w, M. Weber^{ax}, H. Weerts^{bm}, A. Wenger^{v, 5}, N. Vermes^u, M. Wetstein^{bi}, A. White^{bz}, D. Wicke^y, G.W. Wilson^{bf}, S.J. Wimpenny^{av}, M. Wobisch^{bh}, D.R. Wood^{bk}, T.R. Wyatt^{ar}, Y. Xie^{by}, S. Yacoob^{ba}, R. Yamada^{ax}, M. Yan^{bi}, T. Yasuda^{ax}, Y.A. Yatsunenkov^{ai}, K. Yip^{bu}, H.D. Yoo^{by}, S.W. Youn^{ba}, C. Yu^m, J. Yu^{bz}, A. Yurkewicz^{bt}, A. Zatserklyaniy^{az}, C. Zeitnitz^y, D. Zhang^{ax}, T. Zhao^{cd}, B. Zhou^{bl}, J. Zhu^{bt}, M. Zielinski^{bs}, D. Zieminska^{bb}, A. Zieminski^{bb}, L. Zivkovic^{br}, V. Zutshi^{az} and E.G. Zverev^{ak}

^aUniversidad de Buenos Aires, Buenos Aires, Argentina

^bLAFEX, Centro Brasileiro de Pesquisas Físicas, Rio de Janeiro, Brazil

^cUniversidade do Estado do Rio de Janeiro, Rio de Janeiro, Brazil

^dInstituto de Física Teórica, Universidade Estadual Paulista, São Paulo, Brazil

^eUniversity of Alberta, Edmonton, Alberta, Simon Fraser University, Burnaby, British Columbia, York University, Toronto, Ontario, and McGill University, Montreal, Quebec, Canada

^fUniversity of Science and Technology of China, Hefei, People's Republic of China

^gUniversidad de los Andes, Bogotá, Colombia

^hCenter for Particle Physics, Charles University, Prague, Czech Republic

ⁱCzech Technical University, Prague, Czech Republic

^jCenter for Particle Physics, Institute of Physics, Academy of Sciences of the Czech Republic, Prague, Czech Republic

^kUniversidad San Francisco de Quito, Quito, Ecuador

^lLaboratoire de Physique Corpusculaire, IN2P3-CNRS, Université Blaise Pascal, Clermont-Ferrand, France

^mLaboratoire de Physique Subatomique et de Cosmologie, IN2P3-CNRS, Université de Grenoble 1, Grenoble, France

ⁿCPPM, IN2P3-CNRS, Université de la Méditerranée, Marseille, France

^oLaboratoire de l'Accélérateur Linéaire, IN2P3-CNRS et Université Paris-Sud, Orsay, France

^pLPNHE, IN2P3-CNRS, Universités Paris VI and VII, Paris, France

^qDAPNIA/Service de Physique des Particules, CEA, Saclay, France

^rIPHC, Université Louis Pasteur et Université de Haute Alsace, CNRS, IN2P3, Strasbourg, France

^sIPNL, Université Lyon 1, CNRS/IN2P3, Villeurbanne, and Université de Lyon, Lyon, France

^tIII. Physikalisches Institut A, RWTH Aachen, Aachen, Germany

^uPhysikalisches Institut, Universität Bonn, Bonn, Germany

^vPhysikalisches Institut, Universität Freiburg, Freiburg, Germany

^wInstitut für Physik, Universität Mainz, Mainz, Germany

^xLudwig-Maximilians-Universität München, München, Germany

^yFachbereich Physik, University of Wuppertal, Wuppertal, Germany

^zPanjab University, Chandigarh, India

^{aa}Delhi University, Delhi, India

^{ab}Tata Institute of Fundamental Research, Mumbai, India

^{ac}University College Dublin, Dublin, Ireland

^{ad}Korea Detector Laboratory, Korea University, Seoul, Republic of Korea

^{ae}SungKyunKwan University, Suwon, Republic of Korea

^{af}CINVESTAV, Mexico City, Mexico

^{ag}FOM-Institute NIKHEF and University of Amsterdam/NIKHEF, Amsterdam, The Netherlands

^{ah}Radboud University Nijmegen/NIKHEF, Nijmegen, The Netherlands

^{ai}Joint Institute for Nuclear Research, Dubna, Russia

^{aj}Institute for Theoretical and Experimental Physics, Moscow, Russia

^{ak}Moscow State University, Moscow, Russia

^{al}Institute for High Energy Physics, Protvino, Russia

^{am}Petersburg Nuclear Physics Institute, St. Petersburg, Russia

^{an}Lund University, Lund, Royal Institute of Technology and Stockholm University, Stockholm, and Uppsala University, Uppsala, Sweden

^{ao}Physik Institut der Universität Zürich, Zürich, Switzerland

^{ap}Lancaster University, Lancaster, United Kingdom

^{aq}Imperial College, London, United Kingdom

^{ar}University of Manchester, Manchester, United Kingdom

^{as}University of Arizona, Tucson, AZ 85721, USA

^{at}Lawrence Berkeley National Laboratory and University of California, Berkeley, CA 94720, USA

^{au}California State University, Fresno, CA 93740, USA

^{av}University of California, Riverside, CA 92521, USA

- ^{aw}Florida State University, Tallahassee, FL 32306, USA
^{ax}Fermi National Accelerator Laboratory, Batavia, IL 60510, USA
^{ay}University of Illinois at Chicago, Chicago, IL 60607, USA
^{az}Northern Illinois University, DeKalb, IL 60115, USA
^{ba}Northwestern University, Evanston, IL 60208, USA
^{bb}Indiana University, Bloomington, IN 47405, USA
^{bc}University of Notre Dame, Notre Dame, IN 46556, USA
^{bd}Purdue University Calumet, Hammond, IN 46323, USA
^{be}Iowa State University, Ames, IA 50011, USA
^{bf}University of Kansas, Lawrence, KS 66045, USA
^{bg}Kansas State University, Manhattan, KS 66506, USA
^{bh}Louisiana Tech University, Ruston, LS 71272, USA
^{bi}University of Maryland, College Park, MD 20742, USA
^{bj}Boston University, Boston, MA 02215, USA
^{bk}Northeastern University, Boston, MA 02115, USA
^{bl}University of Michigan, Ann Arbor, MI 48109, USA
^{bm}Michigan State University, East Lansing, MI 48824, USA
^{bn}University of Mississippi, University, MS 38677, USA
^{bo}University of Nebraska–Lincoln, Lincoln, NE 68588, USA
^{bp}Princeton University, Princeton, NJ 08544, USA
^{bq}State University of New York, Buffalo, NY 14260, USA
^{br}Columbia University, New York, NY 10027, USA
^{bs}University of Rochester, Rochester, NY 14627, USA
^{bt}State University of New York, Stony Brook, NY 11794, USA
^{bu}Brookhaven National Laboratory, Upton, NY 11973, USA
^{bv}Langston University, Langston, OK 73050, USA
^{bw}University of Oklahoma, Norman, OK 73019, USA
^{bx}Oklahoma State University, Stillwater, OK 74078, USA
^{by}Brown University, Providence, RI 02912, USA
^{bz}University of Texas, Arlington, TX 76019, USA
^{ca}Southern Methodist University, Dallas, TX 75275, USA
^{cb}Rice University, Houston, TX 77005, USA
^{cc}University of Virginia, Charlottesville, VI 22901, USA
^{cd}University of Washington, Seattle, WA 98195, USA

¹ Visitor from Augustana College, Sioux Falls, SD, USA.

² Visitor from The University of Liverpool, Liverpool, UK.

³ Visitor from ICN-UNAM, Mexico City, Mexico.

⁴ Visitor from Helsinki Institute of Physics, Helsinki, Finland.

⁵ Visitor from Universität Zürich, Zürich, Switzerland.

* Corresponding author— email: hobbs@sbhep.physics.sunysb.edu (J. D. Hobbs)

Editor: L. Rolandi.

Abstract

We describe a search for the Standard Model Higgs boson with a mass of 105 GeV/ c^2 to 145 GeV/ c^2 in data corresponding to an integrated luminosity of approximately 450 pb⁻¹ collected with the DØ detector at the Fermilab Tevatron $\bar{p}p$ collider at a center-of-mass energy of 1.96 TeV. The Higgs boson is required to be produced in association with a Z boson, and the Z boson is required to decay to either electrons or muons with the Higgs boson decaying to a $b\bar{b}$ pair. The data are well described by the expected background, leading to 95% confidence level cross section upper limits $\sigma(\bar{p}p \rightarrow ZH) \times (B(H \rightarrow b\bar{b}))$ in the range of 3.1 pb to 4.4 pb.

Over the past two decades, increasingly precise experimental results have repeatedly validated the Standard Model (SM) and the relationship between gauge invariance and the embedded coupling strengths. For massive W and Z bosons, gauge invariance of the Lagrangian is preserved through the Higgs mechanism, but the Higgs boson (H) has

yet to be observed. The current lower bound on the mass of the Higgs boson from direct experimental searches is $M_H = 114.4$ GeV/ c^2 at the 95% confidence level [1]. Searches for $\bar{p}p \rightarrow WH \rightarrow e(\mu)\nu b\bar{b}$, $\bar{p}p \rightarrow WH \rightarrow WWW^*$, and $\bar{p}p \rightarrow ZH \rightarrow \nu\bar{\nu} b\bar{b}$ have been recently reported [2], [3] and [4]. The CDF Collaboration has recently reported results in the $\bar{p}p \rightarrow WH \rightarrow \ell\nu$ channel [5]

and previously reported results in the $p\bar{p} \rightarrow WH \rightarrow \ell\nu$ and $p\bar{p} \rightarrow ZH \rightarrow \ell^+ \ell^- b\bar{b} (\ell = e, \mu)$ channels with significantly smaller data sets [6], [7] and [8]. This Letter provides the first results from the DØ experiment of searches for a Higgs boson produced in association with a Z boson, which then decays either to an electron pair or to a muon pair. The Higgs is assumed to decay to a $b\bar{b}$ pair with a branching fraction given by the SM. The $Z (\rightarrow \ell^+ \ell^-) H$ channels reported in this Letter comprise major components of the search for a Higgs boson at the Tevatron collider.

Z bosons are reconstructed and identified through pairs of isolated electrons or muons with large momentum components transverse to the beam direction (p_T), having invariant mass consistent with that of the Z boson. Events are required to have exactly two jets identified as arising from b quarks (b jets). The resulting data are examined for the presence of a ($H \rightarrow b\bar{b}$) signal in the b -tagged dijet mass distribution. An efficient b -identification algorithm with low misidentification rate and good dijet mass resolution are essential to enhance signal relative to the backgrounds. The analysis of the dielectron [9] (dimuon [10]) channel is based on $450 \pm 27 \text{ pb}^{-1}$ ($370 \pm 23 \text{ pb}^{-1}$) of data recorded by the DØ experiment between 2002 and 2004.

The DØ detector [11] and [12] has a central-tracking system consisting of a silicon microstrip tracker (SMT) and a central fiber tracker (CFT), both located within a ≈ 2 T superconducting solenoidal magnet, with designs optimized for tracking and vertexing covering pseudorapidities $|\eta| < 3$ and $|\eta| < 2.5$, respectively ($\eta = -\ln[\tan(\theta/2)]$, with θ the polar angle relative to the direction of the proton beam). Central and forward preshower detectors are positioned just outside of the superconducting coil. A liquid-argon and uranium calorimeter has a central section (CC) covering pseudorapidities up to $|\eta| \approx 1.1$ and two end calorimeters (EC) that extend coverage to $|\eta| \approx 4.2$, with all three housed in separate cryostats [12]. An outer muon system, covering $|\eta| < 2$, consists of a layer of tracking detectors and scintillation trigger counters in front of 1.8 T toroids, followed by two similar layers behind the toroids [13]. Luminosity is measured using plastic scintillator arrays placed in front of the EC cryostats [14].

The primary background to the Higgs signal is the associated production of a Z boson with jets arising from gluon radiation, among which $Z + b\bar{b}$ production is an irreducible background. The other background sources are $t\bar{t}$ production, diboson (ZZ and WZ) production, and events from multijet production that are misidentified as containing Z bosons. The backgrounds are grouped into two categories with the first category, called physics backgrounds, containing events with Z or W bosons arising from SM processes: inclusive $Z + b\bar{b}$ production, inclusive $Z + jj$ production in which j is a jet without b flavor, $t\bar{t}$, ZZ , and WZ events. This background is estimated from simulation as described below. The second category, called instrumental background, contains those events from multijet production that have two jets misidentified as isolated electrons or muons which appear to arise from the Z boson decay. This background is modeled using control data samples and the procedure described below.

Physics backgrounds are simulated using the leading order ALPGEN [15] and PYTHIA [16] event generators, with the leading order CTEQ5L [17] used as parton distribution functions. The decay and fragmentation of heavy flavor hadrons is done via EVTGEN [18]. The simulated events are passed through a detailed DØ detector simulation program based on GEANT [19] and are reconstructed using the same software program used to reconstruct the collider data. The ZH signal, for a range of Higgs masses, is also simulated using PYTHIA with the same processing as applied to data. Determination of the instrumental background and the normalization of the physics backgrounds are discussed below.

Candidate $Z \rightarrow ee$ events are selected using a combination of single-electron triggers. Accepted events must have two isolated electromagnetic (EM) clusters reconstructed offline in the calorimeter. Isolation is defined as $I = (E_{\text{total}}^{(0.4)} - E_{\text{EM}}^{(0.2)}) / E_{\text{EM}}^{(0.2)}$ in which $E_{\text{total}}^{(0.4)}$ is the total calorimeter energy within $\Delta R < 0.4$ of the electron direction and $E_{\text{EM}}^{(0.2)}$ is the energy in the electromagnetic portion of the calorimeter within $\Delta R < 0.2$ of the electron direction. Candidate electrons must satisfy $I < 0.15$. Each EM cluster must have $p_T > 20 \text{ GeV}/c$ and either $|\eta_{\text{det}}| < 1.1$ or $1.5 < |\eta_{\text{det}}| < 2.5$, where η_{det} is the pseudorapidity measured relative to the center of the detector, with at least one cluster satisfying $|\eta_{\text{det}}| < 1.1$. In addition, the lateral and longitudinal shower shape of the energy cluster must be consistent with that expected of electrons. At least one of the two EM clusters is also required to have a reconstructed track matching the position of the EM cluster energy. Events with a dielectron mass of $75 < M_{ee} < 105 \text{ GeV}/c^2$ form the Z boson candidate sample in the dielectron channel.

Candidate $Z \rightarrow \mu^+\mu^-$ events are selected using a set of single-muon triggers. Accepted events must have two isolated muons reconstructed offline. The muons must have opposite charge, $p_T > 15 \text{ GeV}/c$, and $|\eta| < 2.0$ with muon trajectories matched to tracks in the central tracking system (i.e., the SMT and the CFT), where the central track must contain at least one SMT measurement. In addition, the central tracks are required to have a distance of closest approach to the interaction vertex in the transverse plane smaller than 0.25 cm. Muon isolation is based on the sum of the energy measured in the calorimeter around the muon candidate and the sum of the p_T of tracks within $\Delta R = ((\Delta\phi)^2 + (\Delta\eta)^2)^{1/2} = 0.5$ of the muon candidate normalized by the muon momentum. The distribution of this variable in background multihadron events is converted to a probability distribution such that a low probability corresponds to an isolated muon. The product of the probabilities for both muons in an event is computed, and the event is retained if the product is less than 0.02. Accepted Z boson candidates must have the opening angle of the dimuon system in the transverse plane (azimuth) of $\Delta\phi > 0.4$, and invariant mass $65 < M_{\mu\mu} < 115 \text{ GeV}/c^2$. The $\Delta\phi$ requirement is used to protect against potential residual, difficult to model background from low mass dimuon production in which one of the muons is badly mismeasured. It is present in the preselection but has essentially no impact after the dimuon mass requirement. This mass range differs from that of the dielectrons because of the difference in resolutions of electron energies and muon momenta.

After selecting the Z candidate events, we define a Z + dijet sample which, in addition to satisfying the Z candidate selection requirements, has at least two jets in each event. Jets are reconstructed from energy in calorimeter towers using the Run II cone algorithm with $\Delta R = 0.5$ [20] with towers defined as non-overlapping, adjacent regions of the calorimeter $\Delta\eta \times \Delta\phi = 0.1 \times 0.1$ in size. The transverse momentum of each jet is corrected for multiple $\bar{p}p$ interactions, calorimeter noise, out-of-cone showering in the calorimeter, and energy response of the calorimeter as determined from the transverse momentum imbalance in photon + jet events [21]. Only jets that pass standard quality requirements and satisfy $p_T > 20$ GeV/ c and $|\eta| < 2.5$ are used in this analysis. The quality requirements are based on the pattern of energy deposition within a jet and consistency with the energy deposition measured by the trigger system.

For the $Z \rightarrow ee$ channel, the normalizations of the smaller $t\bar{t}$, WZ and ZZ backgrounds are computed using simulated events and next-to-leading-order (NLO) cross sections. The cross sections were computed using the MCFM [22] program and the next-to-leading order CTEQ6M [23] parton distribution functions. Trigger efficiency, electron identification (ID) efficiency and resolution correction factors are derived from comparisons of data control samples and simulated events. The background contributions from $Z + jj$, $Z + bj$ and $Z + b\bar{b}$ processes are normalized to the observed Z + dijet data yield reduced by the expected contributions from the smaller physics and instrumental backgrounds. The relative fractions of the $Z + jj$, $Z + bj$ and $Z + b\bar{b}$ backgrounds in the Z + dijet sample are determined from the acceptance and selection efficiencies multiplied by the ratios of the NLO cross sections for these processes again computed using MCFM with CTEQ6M parton distribution functions. For the $Z \rightarrow \mu^+\mu^-$ channel, all physics backgrounds are determined using simulated events with NLO cross sections again determined using MCFM and CTEQ6M. Trigger efficiency, muon ID efficiency, and resolution correction factors are derived from comparison of data control samples and the simulated events.

Instrumental backgrounds in both channels are determined by fitting the dilepton invariant mass distributions to a sum of non- Z and Z boson contributions. The Z boson lineshape is modeled using a Breit-Wigner distribution convoluted with a Gaussian representing detector resolution. The non- Z background, consisting of a sum of events from Drell-Yan production and instrumental background, is modeled using exponentials. The ratio of Z boson to non-resonant Drell-Yan production is fixed by the Standard Model.

The (two) jets arising from Higgs boson decay should contain b -flavored quarks, whereas background from Z + jets has relatively few events with b jets. To improve the signal-to-background ratio, two of the jets in the events from the Z + dijet sample are required to exhibit properties consistent with those of jets containing b quarks. The same b -jet identification algorithm [24] is used for the dielectron and dimuon samples. It is based on the finite lifetime of b hadrons giving a low probability that these tracks appear to arise from the primary vertex and considers all central tracks associated with a jet.

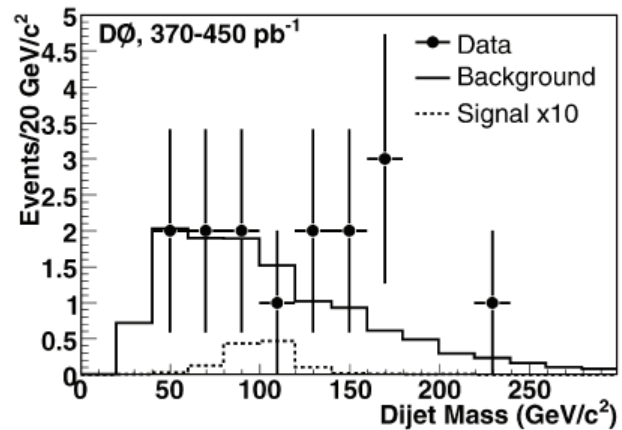


Figure 1. The dijet invariant mass distribution in double-tagged Z + dijet events. The Higgs signal corresponds to $M_H = 115$ GeV/ c^2 . (The uncertainties are statistical only.)

A small probability corresponds to jets with tracks with large impact parameter, as expected in b hadron decays. The efficiency for tagging a b jet from Higgs decay is approximately 50%, determined as described in the next paragraph. The probability of misidentifying a jet arising from a charm quark as a b jet is roughly 20%. The inclusive Z + dijet sample has a $c\bar{c}$ content of roughly 2.3%. The probability to misidentify a jet arising from a light quark (u, d, s) or gluon as a b jet is roughly 4%. This choice of efficiency and purity optimizes the sensitivity of the analysis. The relatively large per-jet light-flavor misidentification rate can be accommodated because two tagged jets are required in each event.

For background yields determined from simulated events, the probability as a function of jet p_T and η that a jet of a given flavor would be identified (tagged) as a b jet is applied to each jet in an event. The probability functions are derived from control data samples [25]. For jets in the simulated events, the flavor is determined from a priori knowledge of the parton that gives rise to the jet. The probability of having two b -tagged jets is defined by convoluting the per-jet probabilities assuming there are no jet-to-jet correlations introduced by the b -tag requirement. The observed number of $Z + 2 b$ -jet events and the predicted background levels are shown in Table 1.

The invariant mass of the two b jets in the $Z + 2 b$ jet sample is shown in Figure 1. This distribution is searched for an excess of events. The peak position in the dijet mass spectrum is expected to be at a lower value than the hypothetical Higgs mass because the jet energy is corrected to reflect the energy of particles in the jet cone without a general correction for the lower b -jet response compared with light jets. If any good muon is within $\Delta R < 0.5$ of the jet, then twice the muon momentum is added to the jet momentum (after applying the standard jet correction). This is an approximation to the energy of both the muon and the accompanying neutrino. The expected contribution from Higgs boson production shown in Figure 1 corresponds to $M_H = 115$ GeV/ c^2 .

Systematic uncertainties for signal and background arise from a variety of sources, including uncertainties on the trigger efficiency, on the corrections for differences between

Table 1. Number of observed and expected background events

Final state	$Z + \geq 2$ jets			2 b tags		
	$Z \rightarrow ee$	$Z \rightarrow \mu^+\mu^-$	$Z \rightarrow \ell^+\ell^-$	$Z \rightarrow ee$	$Z \rightarrow \mu^+\mu^-$	$Z \rightarrow \ell^+\ell^-$
Zbb	9.4	8.3	17.4	2.0	1.3	3.3
Zjj	414	437	851	1.2	2.6	3.8
$t\bar{t}$	2.7	9.6	12.3	0.83	3.1	3.9
$ZZ + WZ$	9.2	21.4	30.6	0.32	0.42	0.74
Instrumental	28.0	16.1	44.1	0.18	0.41	0.59
Total background	463	493	956	4.5	7.8	12.3
Observed events	463	545	1008	5	10	15

Table 2. Systematic uncertainty in background and signal predictions given as the fractional uncertainty on the event totals. The ranges correspond to variations introduced by different processes (background), the dijet mass window requirement (background and signal) and intrinsic differences in kinematics arising from different hypothesized Higgs masses (signal)

Source	Background	Signal
Lepton ID efficiencies	11–16%	11–12%
Lepton resolution	2%	2%
Jet ID efficiency	5–11%	8%
Jet energy reconstruction	10%	7%
b -jet ID efficiency	10–12%	9%
Cross sections	6–19%	7%
Trigger efficiency	1%	1%
Luminosity	3%	6.1%
Instrumental background	2% (ee) 12% ($\mu\mu$)	

data and simulation for lepton reconstruction and identification efficiencies, lepton energy resolution, jet reconstruction efficiencies and energy determination, b -identification efficiency, uncertainties from theory and parton distribution functions for cross sections used for simulated events and uncertainties on the method used for instrumental background estimates. The luminosity measurement has an uncertainty of 6.1%. This uncertainty is applied as systematic uncertainty to the background predictions which are absolutely normalized using simulation and to the luminosity input to the limit calculation. The uncertainties from these sources are shown in Table 2. These are evaluated by varying each of the corrections by $\pm 1\sigma$, by comparing different methods (for the instrumental backgrounds), and by varying the parton distribution functions among the 20 error sets provided as part of the CTEQ6L library. The variations seen for different processes for a given uncertainty arise because of differences among the various background processes and because of intrinsic differences in the kinematic spectra from different Higgs mass hypotheses.

The observed yield is consistent with background predictions. Upper limits on the ZH production cross section are derived at 95% confidence level using the CL_s method [26], a modified frequentist procedure, with a log-likelihood ratio classifier. The shapes of full dijet invariant-mass spectra of the signal and background histogrammed in $5 \text{ GeV}/c^2$ bins are used to produce likelihoods that the data are consistent

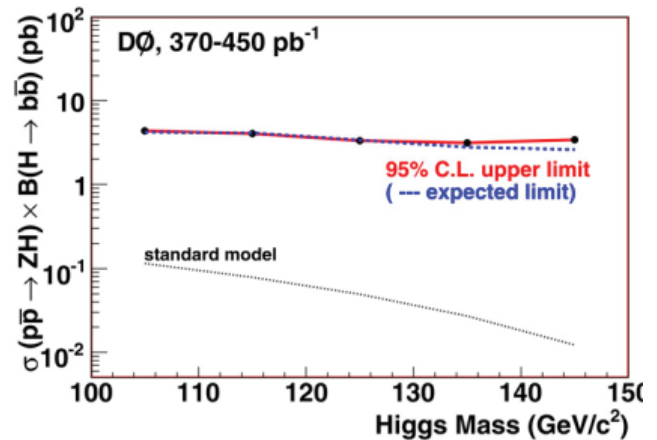


Figure 2. The expected and observed cross-section limits are shown as a function of Higgs mass. The cross section based on the SM is shown for comparison.

with the background-only hypothesis or with a background plus signal hypothesis. Systematic uncertainties are folded into the likelihoods via Gaussian distribution, with correlations maintained throughout. The data yield, predicted backgrounds and expected and observed limits are shown in Table 3 for five hypothetical Higgs masses. The limits are also shown in Figure 2. The mass window in Table 3 is used for illustration. It is centered on the mean of the reconstructed Higgs mass in simulated ZH events and has a width of $\pm 1.5\sigma$ in which σ is the result of a Gaussian fit to the reconstructed dijet mass distribution. The upper bounds differ slightly between the $Z \rightarrow ee$ and $Z \rightarrow \mu^+\mu^-$ events because of different resolutions.

In summary, we have carried out a search for associated ZH production in events having two high- p_T electrons or muons and two jets identified as arising from b quarks. Consistency is found between data and background predictions. A 95% confidence level upper limit on the Higgs boson cross section $\sigma(p\bar{p} \rightarrow ZH) \times B(H \rightarrow b\bar{b})$ is set between 4.4 pb and 3.1 pb for Higgs bosons with mass between $105 \text{ GeV}/c^2$ and $145 \text{ GeV}/c^2$, respectively.

Acknowledgements

We thank the staffs at Fermilab and collaborating institutions, and acknowledge support from the DOE and NSF (USA); CEA and CNRS/IN2P3 (France); FASI, Rosatom and RFBR (Russia); CAPES, CNPq, FAPERJ, FAPESP and

Table 3. Numbers of predicted background and signal events and the observed yield after all selection requirements, including the addition of a dijet mass window. The window is applied for illustration, showing the yields in the region of highest predicted signal-to-background ratio. Also shown are the expected and observed upper limits on the cross section for each channel and for the combined analysis at 95% confidence level computed as described in the text

	$M_H = 105 \text{ GeV}/c^2$		$M_H = 115 \text{ GeV}/c^2$		$M_H = 125 \text{ GeV}/c^2$	
	ee	$\mu\mu$	ee	$\mu\mu$	ee	$\mu\mu$
Mass window (GeV/c^2)	[65, 113]	[65, 118]	[72, 125]	[70, 128]	[75, 136]	[78, 137]
Predicted signal	0.08	0.06	0.06	0.05	0.05	0.03
Background	1.6	3.1	1.7	3.1	1.8	2.8
Data	2	3	1	3	1	4
Expected σ_{95}	5.6	9.9	5.7	8.6	4.5	7.7
Observed σ_{95}	5.4	11.1	4.9	10.5	3.6	11.0
Expected σ_{95}	4.2 pb		4.1 pb		3.4 pb	
Observed σ_{95}	4.4 pb		4.0 pb		3.3 pb	
	$M_H = 135 \text{ GeV}/c^2$		$M_H = 145 \text{ GeV}/c^2$			
	ee	$\mu\mu$	ee	$\mu\mu$		
Mass window (GeV/c^2)	[82, 143]	[84, 147]	[87, 156]	[92, 160]		
Predicted signal	0.027	0.022	0.015	0.01		
Background	1.6	2.9	1.6	2.8		
Data	1	5	0	6		
Expected σ_{95}	4.0	5.5	3.1	7.1		
Observed σ_{95}	3.1	9.3	2.5	13.7		
Expected σ_{95}	2.8 pb		2.6 pb			
Observed σ_{95}	3.1 pb		3.4 pb			

FUNDUNESP (Brazil); DAE and DST (India); Colciencias (Colombia); CONACyT (Mexico); KRF and KOSEF (Korea); CONICET and UBACyT (Argentina); FOM (The Netherlands); PPARC (United Kingdom); MSMT and GACR (Czech Republic); CRC Program, CFI, NSERC and WestGrid Project (Canada); BMBF and DFG (Germany); SFI (Ireland); The Swedish Research Council (Sweden); CAS and CNSF (China); Alexander von Humboldt Foundation; and the Marie Curie Program.

References

- [1] ALEPH Collaboration, DELPHI Collaboration, L3 Collaboration and OPAL Collaboration, *Phys. Lett. B* **565** (2003), p. 61.
- [2] V. M. Abazov *et al.* and DØ Collaboration, *Phys. Rev. Lett.* **94** (2005), p. 091802.
- [3] V. M. Abazov *et al.* and DØ Collaboration, *Phys. Rev. Lett.* **97** (2006), p. 151804.
- [4] V. M. Abazov *et al.* and DØ Collaboration, *Phys. Rev. Lett.* **97** (2006), p. 161803.
- [5] A. Abulencia *et al.* and CDF Collaboration, *Phys. Rev. Lett.* **96** (2006), p. 081803.
- [6] F. Abe *et al.* and CDF Collaboration, *Phys. Rev. Lett.* **79** (1997), p. 3819.
- [7] F. Abe *et al.* and CDF Collaboration, *Phys. Rev. Lett.* **81** (1998), p. 5748.
- [8] D. Acosta *et al.* and CDF Collaboration, *Phys. Rev. Lett.* **95** (2005), p. 051801.
- [9] J. M. Heinmiller, Ph.D. Dissertation, University of Illinois at Chicago, FERMILAB-THESIS-2006-30, 2006.
- [10] H. Dong, Ph.D. Dissertation, Stony Brook University, FERMILAB-THESIS-2007-11, 2007.
- [11] V. M. Abazov *et al.* and DØ Collaboration, *Nucl. Instrum. Methods A* **565** (2006), p. 463.
- [12] S. Abachi *et al.* and DØ Collaboration, *Nucl. Instrum. Methods A* **338** (1994), p. 185.
- [13] V. M. Abazov *et al.* and DØ Collaboration, *Nucl. Instrum. Methods A* **552** (2005), p. 372.
- [14] T. Andeen, *et al.*, FERMILAB-TM-2365-E, April 2007.
- [15] M. L. Mangano, M. Moretti, F. Piccinini, R. Pittau and A. Polosa, *JHEP* **0307** (2003), p. 001.
- [16] T. Sjöstrand *et al.*, *Comput. Phys. Commun.* **135** (2001), p. 238.
- [17] H. L. Lai *et al.*, *Phys. Rev. D* **55** (1997), p. 1280.
- [18] D. J. Lange, *Nucl. Instrum. Methods A* **462** (2001), p. 152.
- [19] R. Brun, F. Carminati, CERN Program Library Long Writeup W5013, 1993.
- [20] G. C. Blazey *et al.* hep-ex/0005012.
- [21] V. M. Abazov *et al.* and DØ Collaboration, *Phys. Rev. D* **74** (2006), p. 092005.
- [22] J. Campbell and K. Ellis <http://mcfm.fnal.gov/>
- [23] J. Pumplin *et al.*, *JHEP* **0207** (2002), p. 12.
- [24] S. Greder, Ph.D. Dissertation, Université Louis Pasteur, Strasbourg, FERMILAB-THESIS-2004-28.
- [25] B. Clement, Ph.D. Dissertation, Strasbourg, IReS, FERMILAB-THESIS-2006-06.
- [26] T. Junk, *Nucl. Instrum. Methods A* **434** (1999), p. 435; A. Read, in: F. James, Y. Perrin, L. Lyons (Eds.), Proceedings of the 1st Workshop on Confidence Limits, CERN-2000-005.